

## PHOTON ENERGY-FLUENCE CORRECTION FACTOR IN LOW-ENERGY BRACHYTHERAPY

Paula C. G. Antunes<sup>1,2</sup>, Javier Vijande<sup>2,3</sup>, Vicent Giménez-Alventosa<sup>2</sup>, Hélio Yoriyaz<sup>1</sup>,  
Facundo Ballester<sup>2</sup>

<sup>1</sup> Instituto de Pesquisas Energéticas e Nucleares (IPEN / CNEN - SP)  
Av. Professor Lineu Prestes 2242  
05508-000 São Paulo, SP  
pacrisguian@gmail.com

<sup>2</sup> Department of Atomic, Molecular, and Nuclear Physics  
University of Valencia  
Burjassot, Spain

<sup>3</sup> Instituto de Física Corpuscular (UV-CSIC)  
University of Valencia  
Burjassot, Spain

### ABSTRACT

The AAPM TG-43 brachytherapy dosimetry formalism has become a standard for brachytherapy dosimetry worldwide; it implicitly assumes that charged-particle equilibrium (CPE) exists for the determination of absorbed dose to water at different locations. At the time of relating dose to tissue and dose to water, or vice versa, it is usually assumed that the photon fluence in water and in tissues are practically identical, so that the absorbed dose in the two media can be related by their ratio of mass energy-absorption coefficients. The purpose of this work is to study the influence of photon energy-fluence in different media and to evaluate a proposal for energy-fluence correction factors for the conversion between dose-to-tissue ( $D_{tis}$ ) and dose-to-water ( $D_w$ ). State-of-the-art Monte Carlo (MC) calculations are used to score photon fluence differential in energy in water and in various human tissues (muscle, adipose and bone) in two different codes, MCNP and PENELOPE, which in all cases include a realistic modeling of the  $^{125}\text{I}$  low-energy brachytherapy seed in order to benchmark the formalism proposed. A correction is introduced that is based on the ratio of the water-to-tissue photon energy-fluences using the large-cavity theory. In this work, an efficient way to correlate absorbed dose to water and absorbed dose to tissue in brachytherapy calculations at clinically relevant distances for low-energy photon emitting seed is proposed. The energy-fluence based corrections given in this work are able to correlate absorbed dose to tissue and absorbed dose to water with an accuracy better than 0.5% in the most critical cases.

### 1. INTRODUCTION

The AAPM TG-43 brachytherapy dosimetry formalism, introduced in 1995 and modified subsequently in various publications [1, 2, 3, 4], has become a standard for brachytherapy dosimetry worldwide. This formalism implicitly assumes that a seed is embedded in an infinite water medium and, consequently, charged-particle equilibrium (CPE) exists. Absorbed dose can, therefore, be approximated by collision kerma. Monte Carlo and experimentally derived TG-43 consensus datasets for both high- and low-energy seed models have been extensively derived in the literature based on these approximations [5, 6, 7].

Currently, most of the clinical experience is mainly based on TG-43, i.e., absorbed dose-to-water in water. However, it is well known that the TG-43 assumptions may not be accurate in some clinical situations [8]. This is particularly true for the combination of low-energy photons ( $< 100$  keV) and some tissues as bone, for which the ratio of mass energy-absorption coefficients are significantly different from unity. The high-Z elements found in bone structures make the photoelectric effect to be the predominant interaction, leading to a higher absorption of low-energy photons and therefore hardening the photon spectrum as it goes deeper on the body [9]. Body-air interfaces, like those observed in breast or lung lesions, are another clinical situation where TG-43 assumptions are not valid [10, 11, 12].

In this context, state-of-the-art model-based dose calculations algorithms (MBDCAs) [13] such as Monte Carlo (MC) and analytical models like ACE (Advanced Calculation Engine – Nucletron – an Elekta Company, Veenendaal, The Netherlands) and ACUROS™ (Transpire Inc., Gig Harbor, WA), both for HDR applications with  $^{192}\text{Ir}$ , have become available in brachytherapy. They are considered by the AAPM Radiation Therapy Committee Task Group 186 (TG-186) as potential replacements of the TG-43 formalism. MBDCAs are capable of handling tissue compositions/densities and other treatments complexities leading to the determination of dose-to-tissue.

The relation between dose-to-tissue and dose-to-water, or vice versa, has been the subject of some recent publications in order to associate all previous clinical experience based on dose-to-water with the new methodologies based on dose-to-tissue [13,14,15,16].

Usually, absorbed dose calculations are performed using cavity theory in which the cavity dimensions are compared to the ranges of secondary electrons [17]. When the cavity is larger than the range of secondary electrons the absorbed dose to non-water tissue is estimated using ratios of mass energy-absorption coefficients between water and tissue [8,10], on the assumption that the photon energy-fluence at the point of interest is practically the same for water and for the different human tissues.

The purpose of this work is to study the influence of photon energy-fluence in different media and to evaluate a proposal for energy-fluence correction factors for the conversion between dose-to-tissue and dose-to-water. For this goal, Monte Carlo simulations using MCNP (Monte Carlo N-Particle) and PENELOPE codes for a subset of human tissues of interest in brachytherapy for  $^{125}\text{I}$  - low energy brachytherapy seed has been performed.

## 2. MATERIALS AND METHODS

This section describes the methodology employed to convert absorbed dose to a tissue ( $D_{tis}$ ) into absorbed dose to water ( $D_w$ ) using the large-cavity theory and how Monte Carlo calculations have been carried out.

### 2.1. Relation between $D_w$ and $D_{tis}$

At this point it should be emphasized that the conversion between  $D_{tis}$  and  $D_w$  is required mainly due to:

- (i) most treatment planning systems (TPS) calculate  $D_w$ , hence available clinical experience is based on  $D_w$ ;
- (ii) advanced developments in absorbed dose calculation methods determine accurately  $D_{tis}$  assuming that a valid characterization of tissues from dual-CT procedures or from a lookup density-tissue table has been made;
- (iii) a comparison between  $D_{tis}$  obtained by Monte Carlo calculations with  $D_w$  calculated with conventional TPS, and their transfer method, is necessary to update  $D_w$ -based previous clinical experience.

TG-43 photon brachytherapy dosimetry assumes that:

- 1) The source is located in an infinite water medium and charged particle equilibrium (CPE) exists (except in the vicinity of the source capsule).
- 2) The absorbed dose to a tissue located in such a water infinite medium,  $D_{tis}$ , at a point is approximated by the collision kerma,  $(K_{col})_{tis}$ , at the same point, i.e.:

$$D_{tis} \stackrel{CPE}{=} (K_{col})_{tis} = \Psi_{tis} (\bar{\mu}_{en} / \rho)_{tis} \quad (1)$$

where  $(\bar{\mu}_{en} / \rho)_{tis}$  is the mass energy-absorption coefficient, averaged over the photon energy-fluence spectrum, and  $\Psi_{tis} = \int_E \Psi_E^{tis} dE$  is the total photon energy-fluence, with:

$$\Psi_E^{tis} = \frac{d\Psi}{dE} \Big|_{tis} = E \Phi_E^{tis} = E \frac{d\Phi}{dE} \Big|_{tis} \quad (2)$$

$\Phi_E^{tis}$  being the photon fluence spectrum, differential in energy, at the point of interest.

- 3) The relation between dose-to-water,  $D_w$ , and dose-to-tissue  $D_{tis}$  can therefore be written as

$$\frac{D_w}{D_{tis}} = \frac{\Psi_w (\bar{\mu}_{en} / \rho)_w}{\Psi_{tis} (\bar{\mu}_{en} / \rho)_{tis}} = \frac{\Psi_w}{\Psi_{tis}} (\bar{\mu}_{en} / \rho)_{tis}^w = \Psi_{tis}^w (\bar{\mu}_{en} / \rho)_{tis}^w \quad (3)$$

where  $\Psi_{tis}^w$  is the ratio of the total photon energy-fluences in water and in tissue, and  $(\bar{\mu}_{en} / \rho)_{tis}^w$  is the ratio of mass energy-absorption coefficients of water and tissue, averaged over the local photon energy-fluence.

- 4) Assuming, as is widely done, that the photon energy-fluence at the point of interest is practically the same in tissue and in water, i.e. that  $\Psi_{tis}^w \cong 1$ , eq. (3) becomes:

$$\frac{D_w}{D_{tis}} = (\bar{\mu}_{en} / \rho)_{tis}^w \quad (4)$$

5) If, on the other hand, the photon energy-fluence depends on the medium at the point of interest, the ratio  $\Psi_{tis}^w$  needs to be taken into account, so that eq. (3) becomes:

$$\frac{D_w}{D_{tis}} = \Psi_{tis}^w (\bar{\mu}_{en} / \rho)_{tis}^w \quad (5)$$

where  $\Psi_{tis}^w$  is the ratio of the total photon energy-fluence in water and tissue, which in this work is termed the water-to-tissue photon energy-fluence correction factor.

This work explores the relations (4) and (5) for various human body tissues in the energy region of interest for an  $^{125}\text{I}$  low energy brachytherapy source.

## 2.2. Monte Carlo calculations

Monte Carlo (MC) calculations were performed using the MCNP6 (Monte Carlo N-Particle) code version 1.0 [18,19] and Penelope MC system version 2014 [20], which accurately model photon and electron interactions in an arbitrary material for the energy range of interest in this work.

MCNP6 calculations uses the ENDF/B cross section photon library [21, 22] which is consistent with the NIST database, as stated by previous studies [23]. All calculations were performed using the MCPLIB84 photon cross-section library and EL03 for electrons [18].

Penelope2014 photon cross-sections are based on the EPDL97 cross sections library including binding effects [24, 25] and additionally include the Impulse Approximation to account for Doppler broadening. Photoelectric cross-sections have been calculated with the program *photoabs* [26]. Electron cross-sections are directly calculated by the Penelope data generation code *pendbase* and, for this work.

A comparison of mass energy-absorption coefficients for different materials using the photon dataset of Penelope and values from other libraries (e.g., the NIST database, used by MCNP) has been described by Andreo et al. [27].

### 2.2.1. Low energy brachytherapy seed

The brachytherapy low-energy seed has been investigated in this study is model 6711  $^{125}\text{I}$  source (GE Healthcare, IL. Marketed by Oncura, Inc). The seed was modeled according to published descriptions [5] and the primary radionuclide spectrum were obtained from the USA National Nuclear Data Center (NNDC) [28]. The mean photon energy is 28.5 keV.

### 2.2.2. Materials and geometry of the Monte Carlo calculations

Figure 1 shows the geometric modeling used for the study, which consists of an “infinite” water sphere ( $R = 30$  cm) containing a spherical shell detector of thickness  $\Delta x = 2$  mm (hatched area) with the seed located at its center. In this study, two different “detector” locations were used. In the first one, the detector was located at a distance  $r = 1$  cm of the seed center, and in the second one at a distance  $r = 5$  cm. These detectors were used to score photon energy-fluence spectra differential in energy and absorbed doses in the MC calculations.

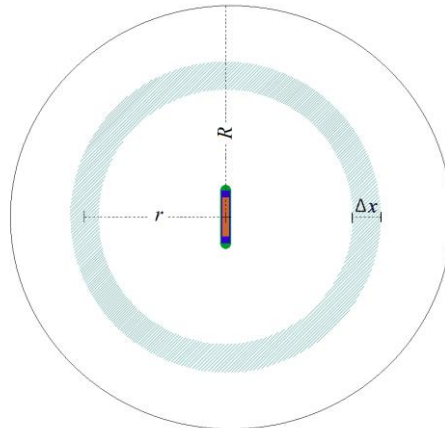


**Figure 1: Schematic illustration of the simulation geometry, the size of the phantom is a water sphere with  $R = 30$  cm, the thickness of the detectors is  $\Delta x = 0.2$  cm, and the source - center to detector distance  $r$  is 1 cm or 5 cm (figure not to scale).**

Water and four human tissues of interest in brachytherapy were considered in the spherical detectors: muscle and adipose tissue composition from ICRP Report 110 [29] and skeletal bone from ICRU Report 46 [30]. The atomic composition and mass density of each material are given in table 1.

**Table 1: Materials compositions (in fraction by weight) and relevant atomic properties**

Material	Water	Muscle	Adipose Tissue	Bone <sub>(ICRU)</sub>
H	$1.12 \cdot 10^{-1}$	$1.01 \cdot 10^{-1}$	$1.19 \cdot 10^{-1}$	$6.39 \cdot 10^{-2}$
C	-	$1.08 \cdot 10^{-1}$	$6.37 \cdot 10^{-1}$	$2.78 \cdot 10^{-1}$
N	-	$2.77 \cdot 10^{-2}$	$7.97 \cdot 10^{-3}$	$2.70 \cdot 10^{-2}$
O	$8.80 \cdot 10^{-1}$	$7.55 \cdot 10^{-1}$	$2.32 \cdot 10^{-1}$	$4.10 \cdot 10^{-1}$
Mg	-	$1.90 \cdot 10^{-4}$	$2.00 \cdot 10^{-5}$	$2.00 \cdot 10^{-3}$
P	-	$1.80 \cdot 10^{-3}$	$1.60 \cdot 10^{-4}$	$7.00 \cdot 10^{-2}$
S	-	$2.41 \cdot 10^{-3}$	$7.30 \cdot 10^{-4}$	$2.00 \cdot 10^{-3}$
Cl	-	$7.90 \cdot 10^{-4}$	$1.19 \cdot 10^{-3}$	-
K	-	$3.02 \cdot 10^{-3}$	$3.20 \cdot 10^{-4}$	-
Ca	-	$3.00 \cdot 10^{-5}$	$2.00 \cdot 10^{-5}$	$1.47 \cdot 10^{-1}$
Others	-	$6.00 \cdot 10^{-5}$	$5.00 \cdot 10^{-4}$	$1.00 \cdot 10^{-4}$
Density (g/cm <sup>3</sup> )	1.0	1.04	0.92	1.85

The  $I$ -values of each material in the codes are given in table 2.

**Table 2:  $I$  – values in eV for different tissues used in PENELOPE and MCNP codes**

	$I$ -value (eV)			
	Water	Muscle	Adipose Tissue	Bone(ICRU)
Penelope	78	75.3	63.2	91.9
MCNP	75.3	75.6	63.2	91.9

Photons and electrons were transported down to an energy cut-off of 1 keV in all simulations. The number of incident photons was set to  $10^9$  for all calculations, so that the Type A standard uncertainty of the MC-scored absorbed dose and total fluence was of the order of 0.5%.

### 2.2.3. Estimators of photon energy-fluence spectra and absorbed dose

Two tallies were employed:

1. Average photon Track length spectra – The “\*F4 + DE/DF” cards in MCNP, which associate the track length with the  $(\mu_{en}/\rho)$  for water and each tissue by NIST; and the “tallyFluenceTrackLength” in Penelope to calculate the average photon track-length spectra within the detector volume, whose output is given multiplied by the detector volume,  $V\Phi_E$ ,  $V$  being the detector volume (the score was subsequently divided by  $V$ ). The *mutren* code of Penelope was used to calculate  $(\mu_{en}/\rho)$  for water and each tissue for the energy of each bin,  $E_i$ .  
Photon fluence spectra  $\Phi_E$  in water and in each tissue, were scored for  $n$  energy bins from  $E_{\min}$  to  $E_{\max}$  the minimum and the maximum energies of each incident seed spectrum (using  $n=158$ ). Subsequently, the energy-fluence differential in energy  $\Psi_E$  was determined from  $\Phi_E$  (see eq. (2)).
2. Absorbed dose - The “\*F8” in MCNP and “tallySphericalDoseDistribution” in Penelope was used to score the absorbed doses  $D_w$  and  $D_{tis}$  inside the two detector volumes.

### 2.3. Ratios of mass energy-absorption coefficients of water and tissue and photon energy-fluence spectra

Using the equations given in section 2.1 together with the MC-scored quantities obtained as described in section 2.2, the energy-fluence weighted average mass energy-absorption coefficient ratios of water and tissue  $(\overline{\mu_{en}/\rho})_{tis}^w$  were evaluated according to:

$$\begin{aligned}
(\bar{\mu}_{en} / \rho)_{tis}^w &= \frac{\int_{E_{min}}^{E_{max}} \Psi_E^w (\mu_{en} / \rho)_w dE}{\int_{E_{min}}^{E_{max}} \Psi_E^w dE} \cong \frac{\sum_{i=1}^n \Psi_{E_i}^w (\mu_{en}(E_i) / \rho)_w}{\sum_{i=1}^n \Psi_{E_i}^w} \\
&= \frac{\int_{E_{min}}^{E_{max}} \Psi_E^{tis} (\mu_{en} / \rho)_{tis} dE}{\int_{E_{min}}^{E_{max}} \Psi_E^{tis} dE} \cong \frac{\sum_{i=1}^n \Psi_{E_i}^{tis} (\mu_{en}(E_i) / \rho)_{tis}}{\sum_{i=1}^n \Psi_{E_i}^{tis}}
\end{aligned} \tag{6}$$

where  $\Psi_{E_i}^w$  and  $\Psi_{E_i}^{tis}$  are the energy-fluence distributions in water and tissue, respectively.

Following the same procedure, the values of the  $\Psi_{tis}^w$ -ratios were calculated using:

$$\Psi_{tis}^w = \frac{\int_{E_{min}}^{E_{max}} \Psi_E^w dE}{\int_{E_{min}}^{E_{max}} \Psi_E^{tis} dE} \cong \frac{\frac{1}{n} \sum_{i=1}^n \Psi_{E_i}^w}{\frac{1}{n} \sum_{i=1}^n \Psi_{E_i}^{tis}} \tag{7}$$

### 3. RESULTS AND DISCUSSION

The calculated mass energy-absorption coefficients of the human tissues relative to those of water are shown in Figure 2(a). For comparison, the quotient between the data from Penelope 2014 and the corresponding NIST-values used by MCNP is presented in figure 2(b). It should be noted that the differences shown are not solely due to the photoeffect cross sections in each dataset, re-normalized in Penelope 2014 and non-re-normalized in NIST, but also to the use of the Impulse Approximation and its account for Doppler broadening in Penelope whereas the NIST data uses the Klein-Nishina kinematics relationship for the scattered photon (Compton line). Both datasets incorporate binding effects.

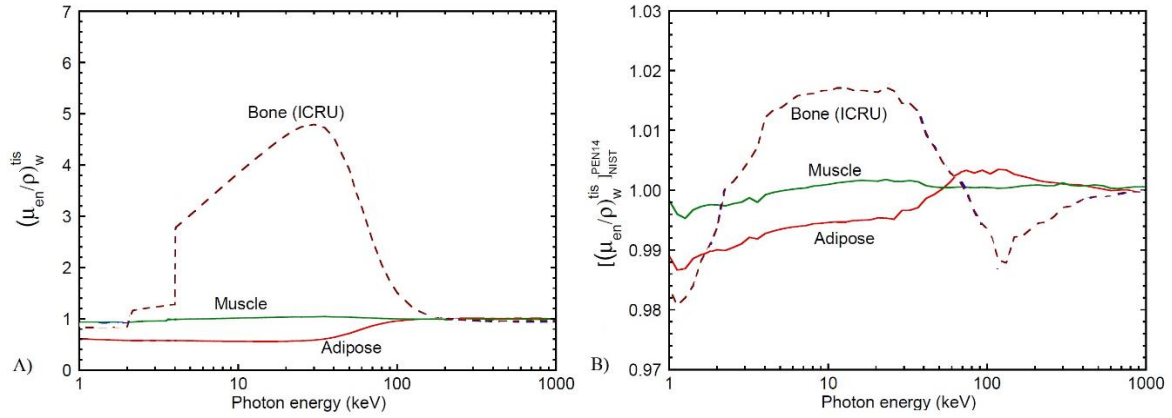


**Figure 2: (a) Mass energy-absorption coefficients of various human tissues relative to water calculated in this work using the *mutren* code of the PENELOPE MC system. (b) ratio of the PENELOPE 2014 quotients to the corresponding NIST values.**

The mass energy-absorptions coefficients values have been used in combination with the photon energy-fluence spectra calculated in the “detectors” at a distance of 1 cm and 5 cm from the seed center. The energy-fluence weighted average mass energy-absorption coefficients ratios were calculated according to equation (6) using the  $E_{min} = 0.5$  keV and  $E_{max} = 35.492$  keV are summarized in table 3.

**Table 3: Energy-fluence weighted average mass energy-absorbed coefficients of different tissue, and their ratio relative to that of water, evaluated for  $^{125}\text{I}$  spectra.**

Materials:	PENELOPE				MCNP			
	1 cm		5 cm		1 cm		5 cm	
	$(\bar{\mu}_{en}/\rho)$ (cm <sup>2</sup> /g)	$(\bar{\mu}_{en}/\rho)_w^{tis}$	$(\bar{\mu}_{en}/\rho)$ (cm <sup>2</sup> /g)	$(\bar{\mu}_{en}/\rho)_w^{tis}$	$(\bar{\mu}_{en}/\rho)$ (cm <sup>2</sup> /g)	$(\bar{\mu}_{en}/\rho)_w^{tis}$	$(\bar{\mu}_{en}/\rho)$ (cm <sup>2</sup> /g)	$(\bar{\mu}_{en}/\rho)_w^{tis}$
Water	0.218	1.000	0.212	1.000	0.215	1.000	0.213	1.000
Muscle	0.227	0.961	0.220	0.961	0.223	0.963	0.219	0.972
Adipose	0.125	1.734	0.122	1.729	0.124	1.728	0.122	0.174
Bone (ICRU)	1.016	0.214	0.982	0.216	0.980	0.219	0.954	0.223

Energy-fluence ratios  $\Psi_{tis}^w$  obtained using equation (7) are given in table 4, where it can be seen that only the muscle/water ratios are approximately close to one. For the two distances, in adipose tissue the energy-fluence ratio to water varies within about -3% and -1%, but it varies up to within 20% and 50% for the ICRU bone composition. Such large differences show that the common assumption of considering approximately equal the fluences in water (or in a soft



tissue like muscle) and in bone, that provides the basis for a dose ratio equal to that of the mass energy-absorption coefficients (see eq. 4), is not acceptable for high-Z tissues.

**Table 4. Energy-fluence weighted average mass photon total energy-fluence and energy-fluence correction factors for different tissues evaluated for  $^{125}\text{I}$  spectra.**

Materials:	PENELOPE				MCNP			
	1 cm		5 cm		1 cm		5 cm	
	$\Psi$ (eV/cm <sup>2</sup> )	$\Psi_{tis}^w$	$\Psi$ (eV/cm <sup>2</sup> )	$\Psi_{tis}^w$	$\Psi$ (eV/cm <sup>2</sup> )	$\Psi_{tis}^w$	$\Psi$ (eV/cm <sup>2</sup> )	$\Psi_{tis}^w$
<b>Water</b>	917.2	1.000	14.19	1.000	896.8	1.000	13.84	1.000
<b>Muscle</b>	915.6	1.002	14.14	1.003	895.2	1.002	13.80	1.003
<b>Adipose</b>	930.0	0.986	14.48	0.979	909,2	0.986	14.13	0.980
<b>Bone (ICRU)</b>	742.1	1.236	10.89	1.302	725.1	1.237	10.66	1.298

The proposal of this work is therefore to include a photon energy-fluence correction factor  $\Psi_{tis}^w$  to account for the fluence difference in two media according to eq. (5). This correction parallels the proposal made by Andreo et al. [31] for megavoltage photon beams, where an electron fluence correction was introduced for the tissues used in the present work. The correction factors are however, substantially larger in the case of low-energy photons used in brachytherapy than in megavoltage photons.

Results for the approximations relating the MC ratio, with the corresponding eq. (4) and eq. (5) at 1 cm and 5 cm, for the spectrum from the  $^{125}\text{I}$  source are given in tables 4 and 5, respectively. It can be seen that the correction of eq. (5) provides dose ratios close to one within a few tenths of a per cent. The results are displayed in Figure 3 for easier visualization.

**Table 4. Data of the approximations relating the MC ratio  $\frac{D_{tis}}{D_w}$  with the corresponding**

**Eq. (4),  $\frac{D_{tis}}{D_w}(\bar{\mu}_{en}/\rho)_{tis}^w$ , and Eq. (5),  $\frac{D_{tis}}{D_w}(\bar{\mu}_{en}/\rho)_{tis}^w \Psi_{tis}^w$  for  $^{125}\text{I}$  spectrum at 1 cm.**

Materials:	1 cm					
	PENELOPE			MCNP		
	$\frac{D_{tis}}{D_w}$	$\frac{D_{tis}}{D_w}(\bar{\mu}_{en}/\rho)_{tis}^w$	$\frac{D_{tis}}{D_w}(\bar{\mu}_{en}/\rho)_{tis}^w \Psi_{tis}^w$	$\frac{D_{tis}}{D_w}$	$\frac{D_{tis}}{D_w}(\bar{\mu}_{en}/\rho)_{tis}^w$	$\frac{D_{tis}}{D_w}(\bar{\mu}_{en}/\rho)_{tis}^w \Psi_{tis}^w$
<b>Muscle</b>	1.038	0.997	0.999	1.037	0.999	1.001
<b>Adipose</b>	0.585	1.015	1.001	0.587	1.015	1.002
<b>Bone (ICRU)</b>	3.761	0.806	0.996	3.726	0.818	1.012

**Table 5. Data of the approximations relating the MC ratio  $\frac{D_{tis}}{D_w}$  with the corresponding**

**Eq. (4),  $\frac{D_{tis}}{D_w}(\bar{\mu}_{en}/\rho)_{tis}^w$ , and Eq. (5),  $\frac{D_{tis}}{D_w}(\bar{\mu}_{en}/\rho)_{tis}^w \Psi_{tis}^w$  for  $^{125}\text{I}$  spectrum at 5 cm.**

Materials:	5 cm					
	PENELOPE			MCNP		
	$\frac{D_{tis}}{D_w}$	$\frac{D_{tis}}{D_w}(\bar{\mu}_{en}/\rho)_{tis}^w$	$\frac{D_{tis}}{D_w}(\bar{\mu}_{en}/\rho)_{tis}^w \Psi_{tis}^w$	$\frac{D_{tis}}{D_w}$	$\frac{D_{tis}}{D_w}(\bar{\mu}_{en}/\rho)_{tis}^w$	$\frac{D_{tis}}{D_w}(\bar{\mu}_{en}/\rho)_{tis}^w \Psi_{tis}^w$
Muscle	1.037	0.997	0.999	1.035	1.006	1.009
Adipose	0.591	1.022	1.001	0.593	1.031	1.010
Bone (ICRU)	3.548	0.766	0.997	3.519	0.786	1.020

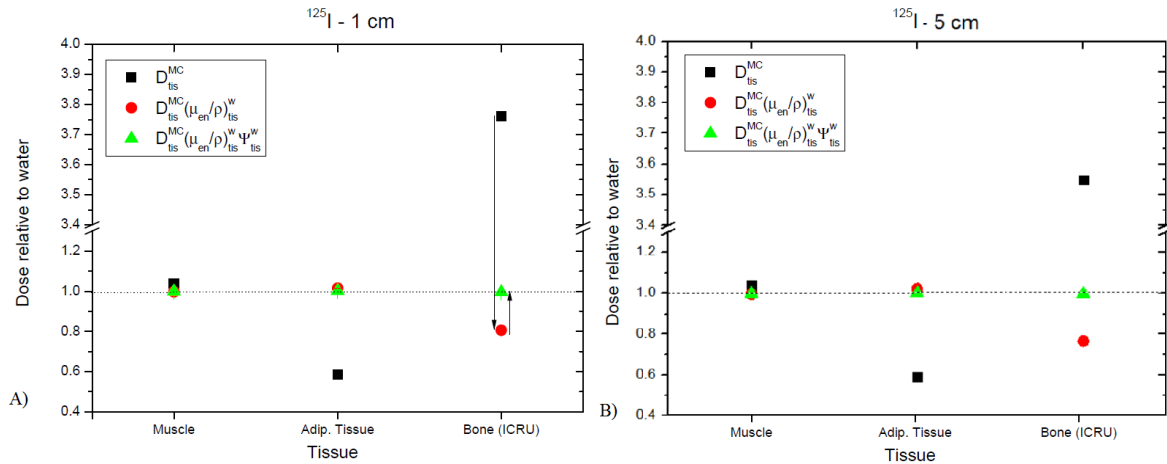


**Figure 3: Ratio between  $D_{tis}$  and  $D_w$  corrected with the approximations given by equations (4) and (5) calculated by MCNP code. The ratios of the Monte Carlo-scored  $D_{tis}$  and  $D_w$  are shown as black squares. The use of the ratio of mass energy-absorption coefficients of water and tissue is shown as red circles. Adding to this ratio the energy-fluence corrections proposed in this work yields the results shown as green triangles. Type A uncertainties for all the absorbed dose ratios are of the order of 0.5%. The arrows in the top-left panel illustrate the trend of dose relative to water when the two different corrections are applied.**

The different dose ratios have been analyzed at 1 cm (the typical prescription distance) and 5 cm (a typical distance for the organs at risk) from the source center in order to distinguish whether the proposed corrections could be used for clinically relevant distances, less than 5 cm from the source.

As expected, significant differences between  $D_w$  and  $D_{tis}$  can be observed for all sources and tissues, especially for bone tissues.  $D_{tis}$  values can be approximately 3.5 times higher than  $D_w$  for the bone tissue. The energy-fluence based correction proposed in Eqs. (5) and (7) provides

an excellent estimation of the correction needed to the ratio  $\frac{D_w}{D_{tis}}$  for the  $^{125}\text{I}$  source used in this work and for all clinically relevant distances with an agreement better than 0.5%.

#### 4. CONCLUSIONS

A photon energy-fluence based correction has been proposed that represents a straightforward and efficient procedure to correlate absorbed dose to water and absorbed dose to tissue in brachytherapy calculations for clinically relevant distances. Its rationale is that photon fluence varies in different media, particularly between water and high-Z tissues like bone; for adipose tissue, the differences are much smaller but still worth correcting for. The corrections provided can be implemented in any treatment planning system and be easily extended to other distances, sources and/or radionuclides by performing a detailed Monte Carlo simulation following the procedures outlined in this work. For the new MBDCa calculation techniques, photon fluence estimators can be included in the calculation process so that both absorbed dose and photon fluence are scored simultaneously; outputs can then be given in terms of dose to tissue and of dose to water in an accurate way.

#### ACKNOWLEDGMENTS

The main author is grateful to acknowledge Capes-Brazil for a research fellowship.

#### REFERENCES

1. Nath, R, L L Anderson, G Luxton, K a Weaver, J F Williamson, and a S Meigooni. "Dosimetry of Interstitial Brachytherapy Sources: Recommendations of the AAPM Radiation Therapy Committee Task Group No. 43. American Association of Physicists in Medicine." *Medical Physics* **22** (2): 209–34. doi:10.1118/1.597458 (1995).
2. Rivard, Mark J, Bert M Coursey, Larry a DeWerd, William F Hanson, M Saiful Huq, Geoffrey S Ibbott, Michael G Mitch, Ravinder Nath, and Jeffrey F Williamson. "Update of AAPM Task Group No. 43 Report: A Revised AAPM Protocol for Brachytherapy Dose Calculations." *Medical Physics* **31** (3): 633–74. doi:10.1118/1.1905824 (2004).
3. Rivard, Mark J. "Brachytherapy Dosimetry Parameters Calculated for a  $^{131}\text{Cs}$  Source." *Medical Physics* **34** (2): 754–62. doi:10.1118/1.2432162 (2007).
4. Rivard, Mark J, Luc Beaulieu, and Firas Mourtada. "Enhancements to Commissioning Techniques and Quality Assurance of Brachytherapy Treatment Planning Systems That Use Model-Based Dose Calculation Algorithms." *Medical Physics* **37** (2010): 2645–58. doi:10.1118/1.3429131 (2010).
5. Dolan, James, Zuofeng Lia, and Jeffrey F Williamson. "Monte Carlo and Experimental Dosimetry of an  $^{125}\text{I}$  Brachytherapy Seed." *Medical Physics* **33** (12): 4675–84. doi:10.1118/1.2388158 (2006).
6. Rivard, Mark J, Stephen D Davis, Larry A DeWerd, Thomas W Rusch, and Steve Axelrod. "Calculated and Measured Brachytherapy Dosimetry Parameters in Water for the Xofigo X-Ray Source: An Electronic Brachytherapy Source." *Medical Physics* **33** (11):

- 4020–32. doi:10.1118/1.2357021 (2006).
7. Perez-Calatayud, Jose, Facundo Ballester, Rupak K. Das, Larry a. DeWerd, Geoffrey S. Ibbott, Ali S. Meigooni, Zoubir Ouhib, Mark J. Rivard, Ron S. Sloboda, and Jeffrey F. Williamson. “Dose Calculation for Photon-Emitting Brachytherapy Sources with Average Energy Higher than 50 keV: Report of the AAPM and ESTRO.” *Medical Physics* **39** (5): 2904–29. doi:10.1118/1.3703892 (2012).
  8. Carlsson-Tedgren, Åsa, and Gudrun Alm-Carlsson. “Specification of Absorbed Dose to Water Using Model-Based Dose Calculation Algorithms for Treatment Planning in Brachytherapy.” *Phys. Med. Biol* **58**: 2561–79. doi:10.1088/0031-9155/58/8/2561 (2013).
  9. Fonseca, Gabriel Paiva, Åsa Carlsson-Tedgren, Brigitte Reniers, Josef Nilsson, Maria Persson, Hélio Yoriyaz, and Frank Verhaegen. “Dose Specification for <sup>192</sup>Ir High Dose Rate Brachytherapy in Terms of Dose-to-Water-in-Medium and Dose-to-Medium-in-Medium.” *Physics in Medicine and Biology* **60** (11): 4565–79. doi:10.1088/0031-9155/60/11/4565 (2015).
  10. Landry, Guillaume, Brigitte Reniers, Jean-Philippe Pignol, Luc Beaulieu, and Frank Verhaegen. “The Difference of Scoring Dose to Water or Tissues in Monte Carlo Dose Calculations for Low Energy Brachytherapy Photon Sources.” *Medical Physics* **38** (3): 1526–33. doi:10.1118/1.3549760 (2011).
  11. Sutherland, J. G. H., K. M. Furutani, Y. I. Garces, and R. M. Thomson. “Model-Based Dose Calculations for <sup>125</sup>I Lung Brachytherapy.” *Medical Physics* **39** (7): 4365. doi:10.1118/1.4729737 (2012).
  12. Afsharpour, Hossein, Guillaume Landry, Brigitte Reniers, Jean-Philippe Pignol, Luc Beaulieu, and Frank Verhaegen. “Tissue Modeling Schemes in Low Energy Breast Brachytherapy.” *Physics in Medicine and Biology* **56** (22): 7045–60. doi:10.1088/0031-9155/56/22/004 (2011).
  13. Beaulieu, Luc, Åsa Carlsson-Tedgren, Jean-François Carrier, Stephen D. Davis, Firas Mourtada, Mark J Rivard, R. M. Thomson, Frank Verhaegen, Todd a. Wareing, and Jeffrey F. Williamson. “Report of the Task Group 186 on Model-Based Dose Calculation Methods in Brachytherapy beyond the TG-43 Formalism: Current Status and Recommendations for Clinical Implementation.” *Medical Physics* **39** (10): 6208–36. doi:10.1118/1.4747264 (2012).
  14. Ballester, Facundo, Åsa Carlsson-Tedgren, Domingo Granero, Annette Haworth, Firas Mourtada, Gabriel Paiva Fonseca, Kyveli Zourari, et al. “A Generic High-Dose Rate <sup>192</sup>Ir Brachytherapy Source for Evaluation of Model-Based Dose Calculations beyond the TG-43 Formalism.” *Medical Physics* **42** (6): 3048–62. doi:10.1118/1.4921020 (2015).
  15. Kumar, Sudhir, Deepak D Deshpande, and Alan E Nahum. “Dosimetric Response of Variable-Size Cavities in Photon-Irradiated Media and the Behaviour of the Spencer–Attix Cavity Integral with Increasing  $\Delta$ .” *Physics in Medicine and Biology* **61** (7). IOP Publishing: 2680–2704. doi:10.1088/0031-9155/61/7/2680 (2016).
  16. Andreo, Pedro. “Dose to ‘Water-Like’ Media or Dose to Tissue in MV Photons Radiotherapy Treatment Planning: Still a Matter of Debate.” *Physics in Medicine and Biology* **60** (1). IOP Publishing: 309–37. doi:10.1088/0031-9155/60/1/309 (2015).
  17. Attix, F. H. “Introduction to Radiological Physics and Radiation Dosimetry”. New York: Wiley (1986).
  18. Briesmeister, J.F., “A general Monte Carlo N-Particle transport code”, in *Los Alamos National Laboratory Report: LA-13709-M*. (2001).
  19. John T Goorley; Michael R James, T.E.B., Forrest B Brown, Jeffrey S Bull, Lawrence J Cox, Joe W Jr Durkee, “Initial MCNP6 release overview - MCNP version 1.0” Los Alamos. NM: Los Alamos National Laboratory (LA - UR-13-22934) (2013).

20. Salvat, F. “*PENELOPE. A Code System for Monte Carlo Simulation of Electron and Photon Transport*”. Edited by Issy-Les-Moulineaux. France: OECD Nuclear Energy Agency (2014).
21. Chadwick, M.B., “ENDF nuclear data in the physical, biological, and medical sciences”. *Int J Radiat Biol.* **88**(1-2): p. 10-4 (2012).
22. White, M.C., “Photoatomic Data Library MCPLIB03: An Update to MCPLIB02 Containing Compton Profiles for Doppler Broadening of Incoherent Scattering”(2012).
23. J, C.N., “An Introduction to the Passage of Energetic Particles through Matter”, ed. F.T.a.F. Boca Raton. (2006).
24. Cullen, D.E., J. H. Hubbell, and L. Kissel. “EPDL97: The Evaluated Photon Data Library.” In *Laboratory, Lawrence Livermore National*, 97 version. Livermore: University of California (1997).
25. Perkins, S.T., D.E. Cullen, and S.M. Seltzer. “Tables and Graphs of Electron-Interaction Cross-Sections from 10 eV to 100 GeV Derived from the LLNL Evaluated Electron Data Library (EEDL) Z=1-100”. *Lawrence Livermore National Laboratory* (2001).
26. Sabbatucci, Lorenzo, and Francesc Salvat. “Theory and Calculation of the Atomic Photoeffect.” *Radiation Physics and Chemistry* **121**. Elsevier: 122–40. doi:10.1016/j.radphyschem.2015.10.021. (2016).
27. Andreo, Pedro, David T Burns, and Francesc Salvat. “On the Uncertainties of Photon Mass Energy-Absorption Coefficients and Their Ratios for Radiation Dosimetry.” *Physics in Medicine and Biology* **57 (8)**: 2117–36. doi:10.1088/0031-9155/57/8/2117 (2012).
28. Baglin, Coral M. “Nuclear Data Sheets for A = 192.” *Nuclear Data Sheets* **113** (8–9). Elsevier Inc.: 1871–2111. doi:10.1016/j.nds.2012.08.001. (2012).
29. ICRP. “Adult Reference Computational Phantoms.” *Annals of the ICRP* **39** (2): 3–5. doi:10.1016/j.icrp.2009.09.001 (2009).
30. ICRU. “Photon, Electron, Proton and Neutron Interaction Data for Body Tissues.” *ICRU Report 46* (February) (1992).
31. Andreo, Pedro, Hugo Palmans, Maria Marteinsdóttir, Hamza Benmakhlouf, and Åsa Carlsson-Tedgren. “On the Monte Carlo Simulation of Small-Field Micro-Diamond Detectors for Megavoltage Photon Dosimetry.” *Physics in Medicine and Biology* **61**: L1–10. doi:10.1088/0031-9155/61/1/L1 (2016).